JOURNAL OF EXPERIMENTAL AND THEORETICAL PHYSICS, 2024, Vol. 165, No. 3, pp. 354–366

SOLID BODIES AND LIQUIDS

CHANGES IN TRANSITION METAL DICHALCOGENIDE FILMS PROPERTIES ON VARIOUS STAGES OF CHEMICAL VAPOR DEPOSITION

© 2024 A.B. Loginov [a*], R.R. Ismagilov [a], P.V. Fedotov [b,c], I.V. Sapkov [a], M.M. Kuvatov [a], B.A. Loginov [d], E.D. Obraztsova [b,c], A. N. Obraztsov [a]

[a] Physics Department, Lomonosov Moscow State University, 119991 Moscow, Russia
[b] Prokhorov General Physics Institute of the Russian Academy of Sciences, 119991 Moscow, Russia
[c] National Research University "Moscow Institute of Physics and Technology", 141701 Dolgoprudny, Russia
[d] National Research University of Electronic Technology, 124498, Zelenograd, Russia

*e-mail: loginov.ab15@physics.msu.ru

Received July 07, 2023
Revised September 21, 2023
Accepted October 02, 2023

Abstract. Transition metal dichalcogenides (TMDs) are attracting continuously growing attention due to a number of their unique properties. Possibilities of their application are significantly defined by improvement of obtaining methods. In this work we study formation of TMD (MoS_2, WS_2) mesoporous films during chemical vapor deposition with the use of gaseous H2S and thermally evaporated transition metals (Mo or W). Morphology, Raman spectra, photoluminescent properties and electrical conductivity of TMD films are investigated at different precursors concentrations and deposition duration times. The analysis revealed main stages of TMD films growth: isolated 2D monocrystalline islands formation (i), partial overlapping of these crystallites with their gradual growth in the plane of the substrate (ii), formation and growth of plate-like crystallites oriented perpendicular to the substrate surface (iv). Qualitative changes of morphology, electrical conductivity and PL properties of TMD films are explained with taking into account interaction of TMD electronic sub-system with the substrate and neighboring crystallites.

Keywords: *transition metal dichalcogenides*, *nanowalls*, *chemical vapor deposition*, *MoS2*, *WS2*, *monolayers*

DOI: 10.31857/S00444510240305e2

1. INTRODUCTION

Transition metal dichalcogenides (TMD) is a class of compounds that, due to their unique properties, have attracted considerable attention in the scientific and technical community in recent decades [1-3]. The crystal lattice of the TMD has a layered structure. A distinctive feature of this structure is that all covalent bonds between the atoms are closed inside the layer, and interlayer communication is realized by weak van-der-Waals interaction, which, in particular, makes it easy to separate layers from each other and use isolated layers for research, to create electronics devices based on TMD monolayers and for other purposes. The chemical formula of TMDs is usually written as MoX_2, where M is a transition metal atom (Mo, W, Re, V, Ta etc.), and X is a halogen (S, Se, Te). A single layer of TMD can be represented in the form of alternating two-dimensional hexagonal structures, two of which are formed by chalcogen atoms, and a third of transition metal atoms is located between them. The resulting structure of the TMD monolayer with such a packing of $X - M - X$ atoms turns out to be devoid of an inversion center, which leads, together with a comparatively large mass of atoms, to the emergence of a number of unique properties (the presence of nonequivalent lines (K and K') in the law of electron dispersion, a new splitting of the valence band, etc.) and it makes it possible to consider such materials as the basis for creating promising spintronics and dolintronics devices [4, 5].

Individual single crystals of TMDs containing one or more layers exhibit pronounced two-dimensional properties. The effects of dimensional quantization associated with the small thickness of such crystallites (up to 10 nm) lead to the manifestation of physical properties due to the two-dimensional nature of the electron gas in these structures [6, 7]. In particular, significantly reduced dielectric screening leads to an increase in the binding energy of the bound states of electrons and holes and leads to the possibility of the existence of excitons and trions (and the observation of related effects) at room temperatures, which opens the way to their practical use [8,9]. The replacement of the type of transition atoms in the chemical structure with a little-changing crystal lattice can radically change the properties of TMDs. Thus, depending on the number of d-electrons in the transition atom, the zones in the electron spectrum are filled in various ways, and the TMDs can exhibit both metallic and semi-semiconductor or dielectric properties. The combination of various types of TMDs with a similar crystal lattice leads to the formation of epitaxial heterojunctions, which can be used in various electronic devices [10-12].

TMDs are of particular interest for optoelectronics. When the number of layers in a crystal is reduced to one, semiconductor TMD move from the non-direct band state to the direct band, as a result of which the frequency of electronic transitions and the efficiency of the corresponding processes associated with the absorption or emission of photons increase many times. For example, the MoS_2 monolayer (one of the most common representatives of TMDs) can absorb up to 20% of the light radiation that affects it in a certain wavelength range [13, 14]. The morphology of the studied samples has an important influence on the properties of TMD. The overwhelming number of works is concentrated on the study and application of films or separate crystallites of TMD, the planes of atomic layers in which are parallel to the substrate (the so-called planar crystallites) [15-17]. However, since the properties of the TMD of a crystallite depend, among other things, on its environment (for example, on the characteristics of the substrate in contact with it), TMD films consisting of crystallites, whose atomic layers are oriented perpendicular to the substrate, and the contact between them is limited to a relatively small area, represent a certain interest. These crystallites are called “vertically oriented” crystallites. Films consisting of a large number of such vertically oriented crystals have a higher specific surface area and volume of material per unit area of the substrate compared to planar layers, which can significantly and qualitatively improve some parameters of devices created on their basis [18, 19].

One of the simplest (and most widely used to date) methods for producing various two-dimensional materials, including TMDs, has become the method of mechanical exfoliation of a bulk crystal [20]. The TMD planar crystallites obtained in this way have dimensions up to several tens of micrometers and have the best structural quality compared to other methods. The method of mechanical exfoliation is widely used in the study of the fundamental properties of planar TMD structures, however, it is not suitable for use in industrial production due to poor reproducibility of the results and the impossibility of scaling such a technology.

The CVD (Chemical vapor deposition) method is currently considered as one of the most promising alternative methods for the production of thin-film transition metal dichalcogenides [21]. Using this method, it is possible to synthesize materials with a sufficiently high degree of purity, controlled by morphology and chemical composition. The CVD process consists in the formation of materials as a result of a chemical reaction occurring on the surface of a substrate in contact with a gas phase containing the necessary precursors. To obtain TMDs, precursors containing transition metals and chalcogens are introduced into the reaction chamber, usually by thermal decomposition of the resulting reagents. The advantages of the method of chemical deposition from the gas phase include the ability to control the thickness of the film, its structure and chemical composition, as well as the ability to precipitate over large areas and surfaces of various profiles.

The development of this method is necessary to improve the technology of production of TMD-based electronics and optoelectronics devices, such as transistors, solar cells, LEDs and others [10, 12, 22]. The morphology of TMD films, which significantly affects all their properties and the possibility of application, strongly depends on the parameters of CVD synthesis. Despite the widespread use of the CVD method, the synthesis parameters in most cases are chosen empirically based on fairly

general initial concepts. In particular, in this regard, it seems necessary to investigate the mechanisms of formation of TMD films, including the identification of the relationship between changes in their physical properties and the parameters of the synthesis processes used. A detailed study of the process of forming TMD films is also necessary to develop methods for controlled changes in the physical properties, morphology and structural features of the materials obtained.

This paper presents the results of an experimental study of the formation of MoS_2 and WS_2 films in order to identify the peculiarities of changes in their morphological and physical properties when using a new type of CVD synthesis technique proposed by us [23], including the use of gaseous hydrogen sulfide and thermally decomposable Mo or W. The structural and morphological properties and composition of the obtained film materials were analyzed using scanning electron microscopy (SEM), Raman spectroscopy (RAMAN) and fluorescence (FL) spectroscopy. The electrical conductivity of the samples of the obtained films was also studied.

2. EXPERIMENTAL PART

For the synthesis of MoS_2 and WS_2 films, a new variation of the CVD method was used, which we presented earlier [23]. A distinctive feature of this method is the use of gaseous hydrogen sulfide and metallic molybdenum or tungsten in the form of thin filaments as initial reagents.

The reaction chamber with a volume of 5 litres is pre-pumped by a two-stage rotary vane vacuum pump to a pressure of $8.0 \cdot 10^{-3}$ mbar. Hydrogen sulfide flows into the reaction chamber through a needle flow control device. The pressure level in the reaction chamber, controlled by a Pirani sensor, is achieved by equalizing the pumping speeds set by the pre-vacuum pump and the intake of hydrogen sulfide through a controlled leak. The synthesis of all samples studied in this work was carried out at a hydrogen sulfide pressure in a chamber of $8.0 \cdot 10^{-1}$ mbar. The flow of hydrogen sulfide entering the chamber through a quartz tube is directed to a system of parallel filaments made of Mo or W. The filaments are attached to metal holders and heated by an electric current flowing through them of

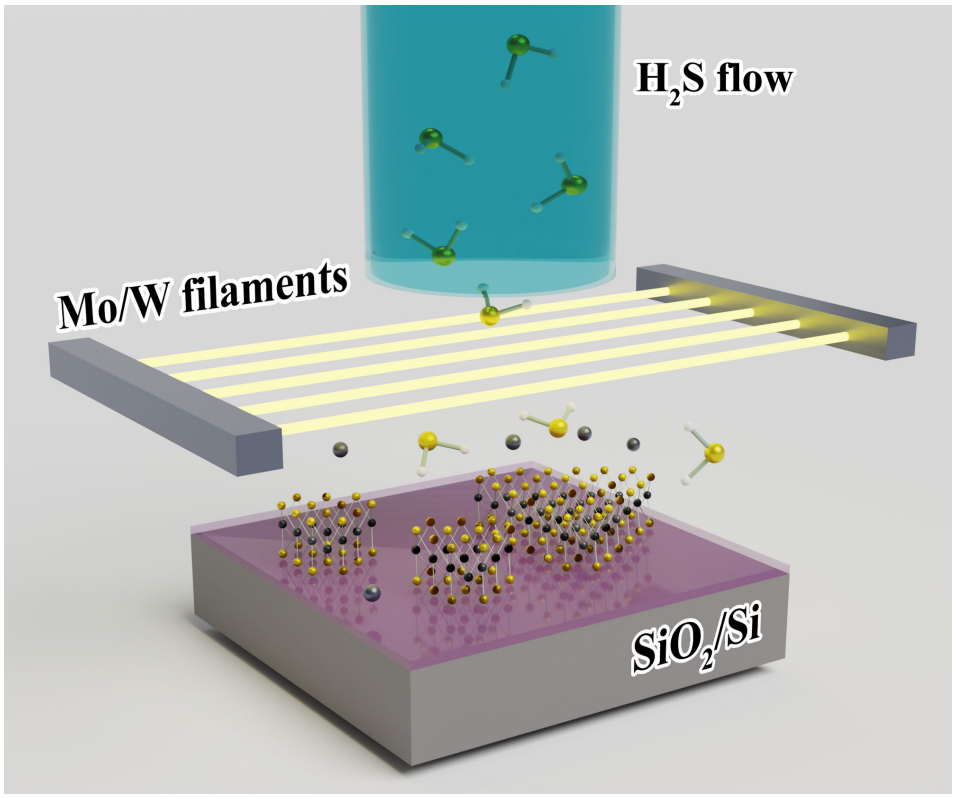

Fig. 1. The scheme of the method of CVD synthesis of TMD films (MoS_2 or WS_2) used in the work on a substrate in the form of oxidized silicon using hydrogen sulfide gas (H_2S) as pre-cursors and obtained by thermal spraying of metal filaments (Mo or W, respectively)

500–900 mA per filament to a temperature ranging from 1000 to 2000 °C. The temperature of the filaments is controlled using an optical pyrometer through the glass lid of the reaction chamber. As a result of the gradual thermal evaporation of the heated filaments, a gaseous stream of metal atoms is created, entrained by a stream of hydrogen sulfide. Hydrogen sulfide blowing on heated filaments partially decomposes into hydrogen and sulfur. The substrate is positioned perpendicular (or at an angle of up to 40°) to the total gas flow at a predetermined distance of 5°–30 mm from the filaments. The substrate is attached to a silicon wafer, which also acts as a heater.

Resistive heating of the silicon wafer during current transmission allows the temperature of the substrate fixed on it to be set at a selected level from room temperature to 1300 °C. The temperature of the substrate is also controlled by an optical pyrometer. At the same time, the heterogeneity of the temperature distribution over the substrate surface was taken into account using the technique presented in [24].

Figure 1 schematically shows the method of deposition of TMD films using CVD synthesis in a mixture of metal vapor (Mo or W) and hydrogen sulfide (H_2S), activated by contact with heated metal filaments. The example shown in Fig. 1 shows the use of oxidized silicon (Si(100)) with an oxide layer thickness (SiO_2) of 300 nm as substrate. Other types of substrates were also used in the work: polished Si plates with a crystallographic orientation of the surface (100) and (111); fused quartz plates; fused quartz plates with a 3 nm thick molybdenum film deposited by magnetron sputtering; freshly ground mica; polycrystalline corundum ceramics with a size of grains 1–10 microns; the same ceramic with a layer of Pt deposited electrolytically.

The possibility of a rapid (characteristic time of the order of 1 s) and independent change in the concentrations of precursors in the gas mixture significantly distinguishes the method used from the traditional one using precursors formed, for example, by the decomposition of powdered S and MoO_3 or WO_3 [25]. One of the results of this advantage was the short duration of the formation of a continuous MoS_2 coating, which was about 15 seconds, which is an order of magnitude less than, for example, with the traditional method [25]. Also, the technique used provides the possibility of controlled deposition and, accordingly, the study of the process of film formation, including changes in their structural and morphological features, at the earliest stages, which was used in the current work. The rate of formation of a continuous coating in the CVD synthesis configuration used by us is determined by metal flows entering the reaction zone on the substrate surface (determined by the evaporation rate of metallic filaments and depends, in particular, on their temperature) and hydrogen sulfide, as well as on the distance between the substrate and the filaments. At the same time, as will be shown below, the deposition results are weakly dependent on the material and temperature (in the range 500–800 °C) of the substrate.

To identify and study the various stages of the formation of MoS_2 and WS_2 films, several series of CVD synthesis experiments were conducted, differing from each other in the temperature of the filaments, the flow of hydrogen sulfide and the distance from the filaments to the substrate at a constant substrate temperature of 780 °C. The obtained film samples were studied using a scanning electron microscope (SEM, Supra 40, Carl Zeiss) equipped with a confocal optical microscope of a Raman spectroscopy meter (HORIBA LabRam HR Evolution UV-VIS-NIR-Open) with an Nd : YAG (532 nm, 14 MW) and a spectrometer for measuring photoluminescence (Horiba Jobin-Yvon Nano-Log-4), equipped with an InGaAs CCD detector (for operation in the range of 850–1600 nm) and an R928P FEU (for operation in the range 180–850 nm). The electrical conductivity of the films was measured using a Keithley 6487 pico ammeter.

3. RESULTS AND DISCUSSION

The composition of the deposition products obtained in the course of the conducted studies was determined by the material of the metal filaments used (Mo or W). Fig. 1 shows the characteristic SEM images of MoS_2 films obtained with a variation in the deposition duration from 15 to 120 s. According to the data of previous studies [23], as well as in accordance with the results of Raman spectroscopy given below, the composition of the obtained films corresponds to MoS_2. In these experiments, single crystal Si plates with an oxide layer 300 nm thick were used as a substrate. The temperature of the substrates was maintained at 780 ° C.

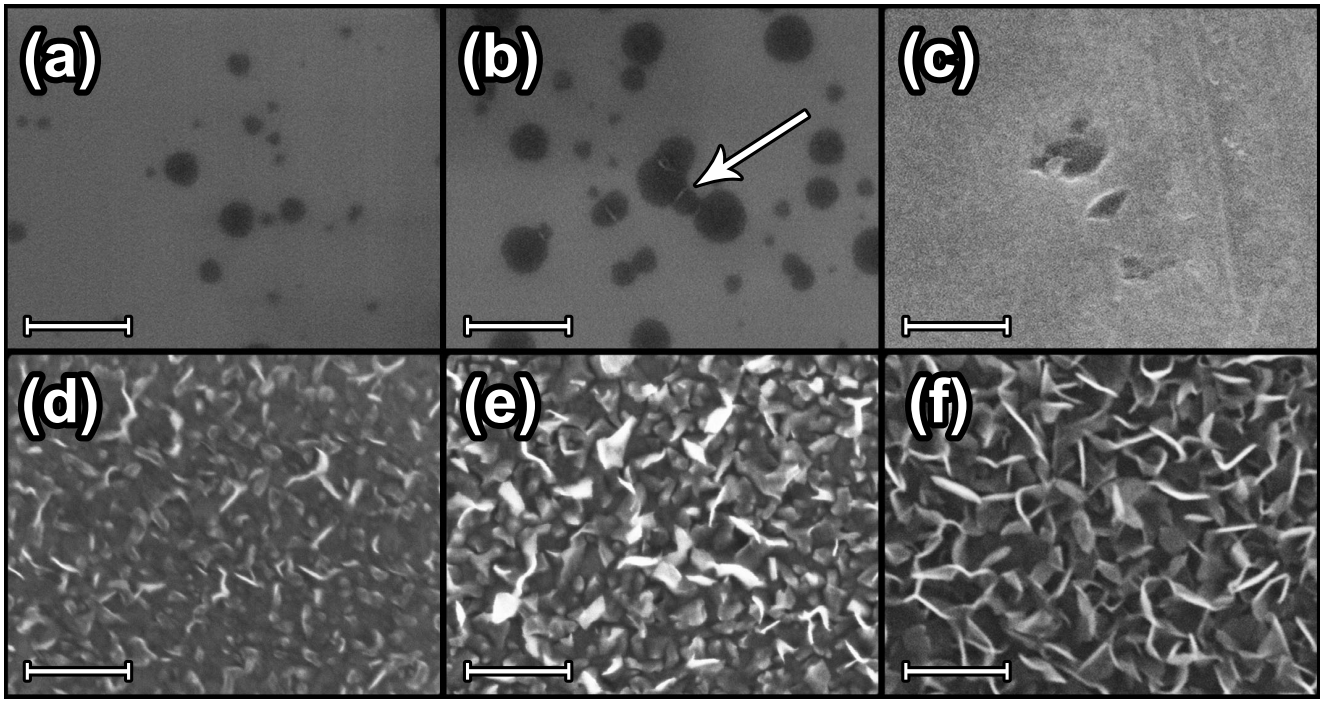

Fig. 2. SEM images of MoS_2 material obtained on oxidized silicon substrates at various durations of the CVD synthesis process: *a*, *b* – the duration of the process is 5 minutes, the incandescent current is 0.77 A per strand, the distance between the substrate and the filaments is 6 and 5 mm, respectively; *c*, *d*, *e*, *f* — current the filament is 0.83 A per filament, the distance between the substrate and the filaments is 5 mm, the deposition duration is 15, 30, 60, 120 seconds, respectively. The arrow indicates the place of formation of a vertically oriented crystallite. The images were obtained at the same scale, the scale segment in all images is 300 nm

A current of 0.83 A flowed through each of the seven molybdenum filaments with a thickness of 60 microns, which led to their heating to temperatures of the order of 1500 ° C. The hydrogen sulfide flow was set in such a way that the pressure in the chamber pumped out by the smart pump was $8.0 \cdot 10^{-1}$ mbar. The distance from the molybdenum filaments to the substrate is 5 mm. It can be seen from the SEM images that even with a minimum deposition time of 15 seconds, an almost continuous coating in the form of a smooth film is formed on the surface of the substrate without obvious signs of morphological protrusions (Fig. 2*c*). With an increase in the deposition time, formations protruding above the main smooth surface, oriented perpendicular to the substrate, were observed. Plate shape and orientation of such formations relative to the substrate becomes more pronounced with an increase in the duration of the deposition process (Fig. 2 *d*, *e*, *f*). At 120 sec duration, plate formations of nanometre thickness reach lateral dimensions (along and perpendicular to the substrate surface) of 100–200 nm (Fig. 2*f*). To study the earlier stages of the formation of the MoS_2 film, CVD synthesis experiments were conducted in which, to reduce the deposition rate, the current flowing through each of the seven molybdenum filaments was reduced to 0.77 A.

With such a filament current and a distance of 6 mm between the filaments and the substrate, coatings were formed in 5 minutes, the characteristic morphology of which is shown in Fig. 2a. As seen from the SEM image shown in this figure, the deposited material consists of islands of a flat shape isolated from each other with transverse dimensions of 50 –150 nm. Some of the islands have a shape corresponding to the crystalline structure of MoS_2. At the same height, but with a decrease in the distance between the filaments and the substrate to 5 mm (Fig. 2b), the deposition rate increased, and the morphology of the film changed. With an increase in the duration of deposition, a gradual merging of the islets is observed. At the same time, linear structures are formed in the places of their contact, which, after filling the main part of the substrate surface, apparently become the centers of nucleation of lamellar formations oriented perpendicular to the substrate and observed, for example, in Fig. 2 *d*, *e*, *f*.

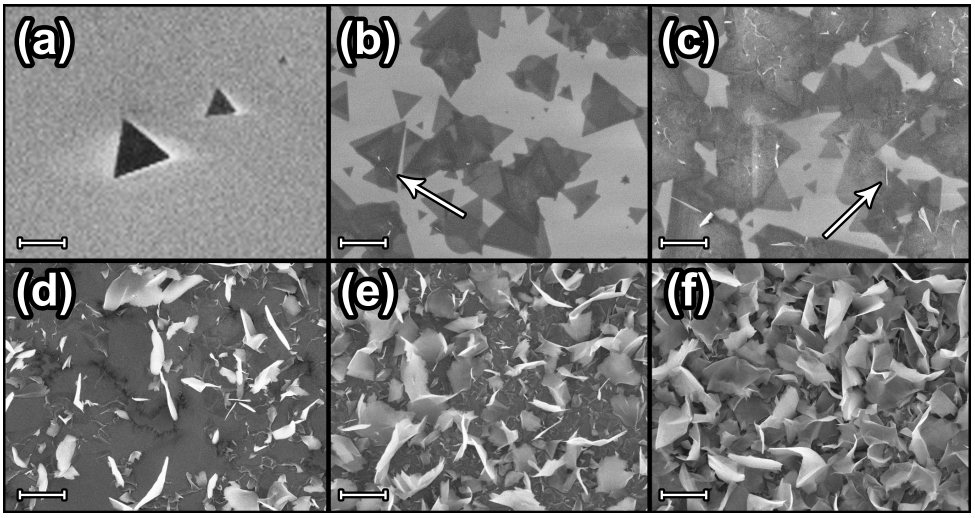

Fig. 3. SEM images of WS_2 material obtained during synthesis, carried out at different distances between the W- filaments and the substrate: 5 mm (*a*); 4.6 mm (*b*); 4.2 mm (*c*); 3.8 mm (*d*). 3.4 mm (*e*); 3 mm (*f*). The arrows indicate the places of formation of vertically oriented crystallites. All images are presented at the same scale, the scale segment is 1 micron

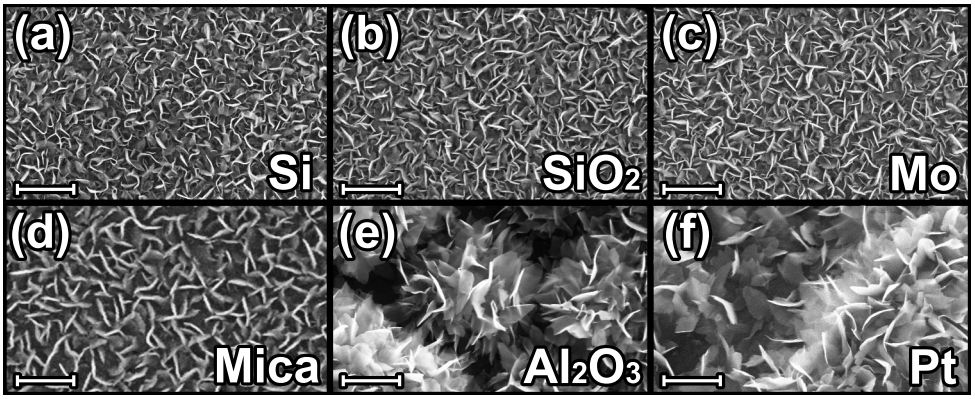

Fig. 4. SEM images of MoS_2 films obtained on different substrates using the same parameters of the CVD process: polished Si plates (*a*); fused quartz plates (*b*); Mo on fused quartz (*c*); freshly cast mica (*d*); corundum polycrystalline ceramics Al_2O_3 (*e*); Pt on corundum ceramics (*f*). All images are presented at the same scale, the scale segment is 500 nm

Similar changes in the morphology of films during deposition were observed during synthesis using tungsten filaments with a diameter of 10 μm. microns. Due to the lower vapor pressure of the evaporated metal (W) [26], such filaments had to be heated to high temperatures of the order of 1700 °C, passing a current of 0.42 A through each of the seven filaments. Fig. 3 shows SEM images of the obtained WS_2 films, the deposition process of which took place on substrates whose plane was located at an angle to the plane of the filaments. Thus, the effect of the distance between the substrate and the niches on the deposition rate and, as a result, on the morphology of the film could be determined on each of the samples. Si plates with an oxide layer of 300 nm thickness were also used as substrates. The temperature of the substrates was set to 920 ° C, the pressure of hydrogen sulfide in the chamber was $8.0 \cdot 10^{-1}$ mbar, the synthesis time was 8 min. At such parameters, in those areas on the substrate, the distance to which from the tungsten filaments was the maximum (5 mm), the growth of individual WS_2 crystallites of regular triangular shape with lateral dimensions of about 1 μm was observed (Fig. 3a). With a decrease in the distance to the filaments (i.e., at a higher deposition rate), the WS_2 crystals, as in the case of MoS_2 (see Figure 2 *d*), began to "collide" with each other, which finally led

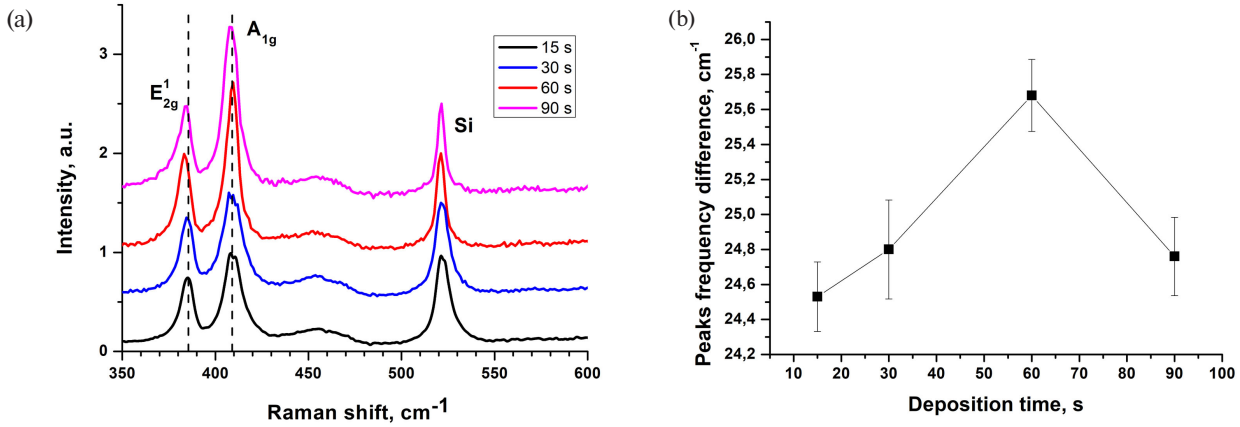

Fig. 5. *a* — Raman spectra of MoS_2 material obtained at different deposition durations. The spectra are normalized to the intensity of the 520 cm^{-1} line corresponding to crystalline silicon. For clarity, the spectra are shifted in the vertical direction. *b* is the dependence of the distance between the Raman peaks of MoS_2 on the duration of deposition

to the formation of a solid film, and the linear structures formed at the points of contact of the islands of two-dimensional WS_2were used as nucleation for the subsequent formation of lamellar crystals oriented perpendicular to the surface of the substrate (Fig. 3 *b*,*c*).

In the areas of the substrate located at shorter distances to the filaments, the film completely covered the substrate and there was a pronounced growth of vertically oriented crystallites (walls) from their nucleation sites on inter-island (intergranular) boundaries. A significant difference in the growth dynamics of WS_2 films compared to MoS_2 was a significantly lower rate of formation of initial islands. The size of the WS_2 crystallites, before they began to come into contact with each other, was about 1 μm, and the crystallites managed to acquire a regular triangular shape. The size of the MoS_2 crystals before their fusion was almost an order of magnitude smaller and averaged about 150 nm.

Experiments on the deposition of MoS_2 films were also carried out using substrates prepared from various materials, differing in composition, crystallographic orientation and degree of surface roughness. The following substrates were used: polished Si plates with crystallographic orientation along the top (100) and (111); Si(100) plates with an oxide layer 300 nm thick; fused quartz plates; fused quartz plates with a 3 nm thick molybdenum film deposited by magnetron sputtering; freshly ground mica; polycrystalline corundum ceramics with a size of rum grains 1 - 10 μm; the same ceramic with a layer of Pt applied electrolytically. The synthesis process took place at substrate temperatures of 500–700 °C, at an incandescent current of 0.83 A molybdenum filaments, a distance of 5 mm from the substrate surface to the filaments, a hydrogen sulfide pressure of $8.0 \cdot 10^{-1}$ mbar and a deposition time of 7 min. As it follows from the SEM images, some of which are shown in Fig. 4, the morphology of the films obtained under these conditions was approximately the same for all types of substrates, regardless of the composition of the material and the degree of roughness (the roughness of corundum ceramics and electrolytically deposited platinum was significantly higher than that of substrates of other types). When trying to use metallic Ni as a substrate instead of deposition of a MoS_2 film, nickel sulfidation with the formation of NiS. Resistance to hydrogen sulfide at temperatures of 500–800 °C is probably the only limitation when choosing spoons for producing MoS_2 films. If this condition is met, the substrate material does not significantly affect the mechanism of formation of MoS_2 films.

This, in particular, can serve as a basis for the possibility of generalizing the results of studies conducted by various methods (Raman spectroscopy, PL, measurement of electrical resistance) for films grown on different substrates, selected for reasons of convenience of implementing each specific technique.

The results of the SEM studies revealed morphological changes in the material obtained during deposition, which indicate the presence of certain stages in the formation of TMD films,

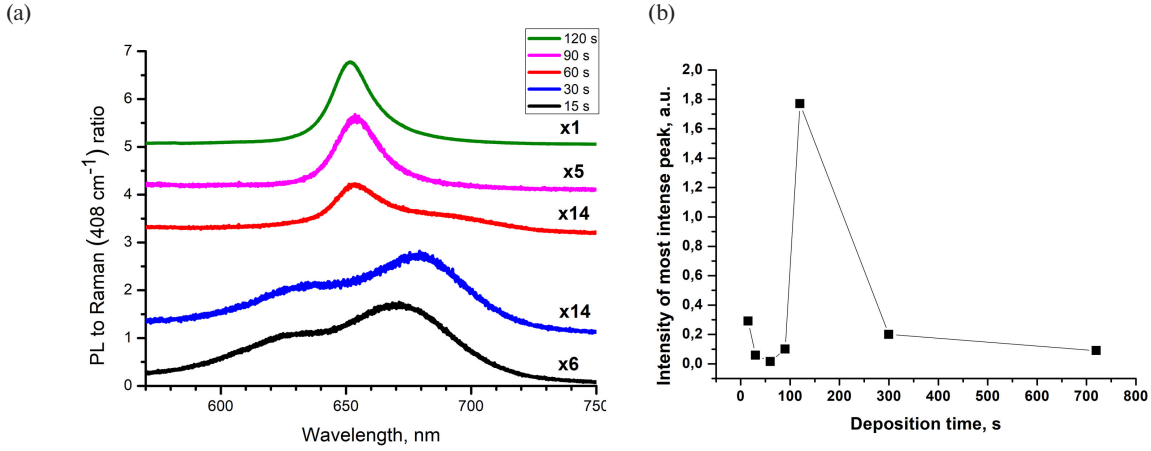

Fig. 6. *a* — Spectra of MoS_2 PL films obtained at different deposition times (for clarity, the spectra are shifted vertically relative to each other, and the normalization coefficients are indicated next to the corresponding curves). *b* is the dependence of the intensity of the most intense PL peak on the deposition time

the same for both types. Such similarity of the morphological characteristics of these materials, as well as the morphology of mesoporous nanographite films, also obtained using CVD [27], can be explained by their layered atomic structure. The MoS_2 samples corresponding to different stages of film growth were also studied by the Raman spectroscopy method. As an example, the Raman spectra for a material obtained on substrates of polished Si at deposition durations of 15, 30, 60, 90 seconds are shown in Fig. 5a. The spectra were normalized to the intensity of the 520 cm^{-1} line corresponding to silicon. At the same time, in Fig. 5, the spectra are shifted in the vertical direction for clarity. These spectra show the characteristic MoS_2 lines (E^1_{2g}- and A_{1g}-modes), located at frequencies 383 and 407 cm^{-1}, as well as the Raman line of silicon (521 cm^{-1}), from which the substrate was made [18]. With an increase in the deposition duration, an increase in the intensity of the MoS_2 lines and a slight shift of their maxima relative to each other and to the Si line in the Raman spectra were observed. Figure 5b shows the dependence of the distance between the maxima of the MoS_2 lines on the duration of the stay. Taking into account the fact that the position of the maxima of the MoS_2 Raman lines is determined, among other things, by the number of atomic layers [18], the data presented in Fig. 5b indicate a non-linear dependence of the number of atomic layers in the MoS_2, crystallites composing the obtained material on the duration of the deposition process: at the initial stage, the thickness of the crystallites increases from about 2–3 to 4–5 atomic layers, and then, after 60 seconds, the number of layers decreases.

This relationship between the number of layers and the position of the Raman spectroscopy lines correlates with SEM observations, in which at the initial stages there is a formation and a gradual increase in the transverse dimensions and thickness of lamellar crystallites while maintaining the predominantly horizontal position of their constituent atomic layers. At the second stage, the formation and growth of MoS_2 crystallites formed by atomic layers oriented vertically (i.e. perpendicular to the substrate) with a smaller thickness corresponding to 2–3 layers is advantageous.

Together with the measurement of the Raman spectra, the spectra of PLMoS_2 films were also recorded, the characteristic examples of which are shown in Fig. 6a. The PL spectra were normalized in intensity to a maximum of the 408 cm^{-1}. Such normalization makes it possible to take into account the additive contribution to the intensity of PL, determined by the volume of material falling into the excitation region. As can be seen in Fig. 6a, the normalized PL spectra change significantly as the deposition duration increases. The normalization coefficients are shown in the figure for each of the spectra. At short deposition durations (15 –30 s) two bands with a maximum at wavelengths of 632 and 680 nm are visible in the PL spectra. According to the literature data, such PL bands are associated with a B-exciton [28] and an A-exciton (trion) [29]. With a further increase in the deposition time, the PL spectrum changes significantly: a peak occurs

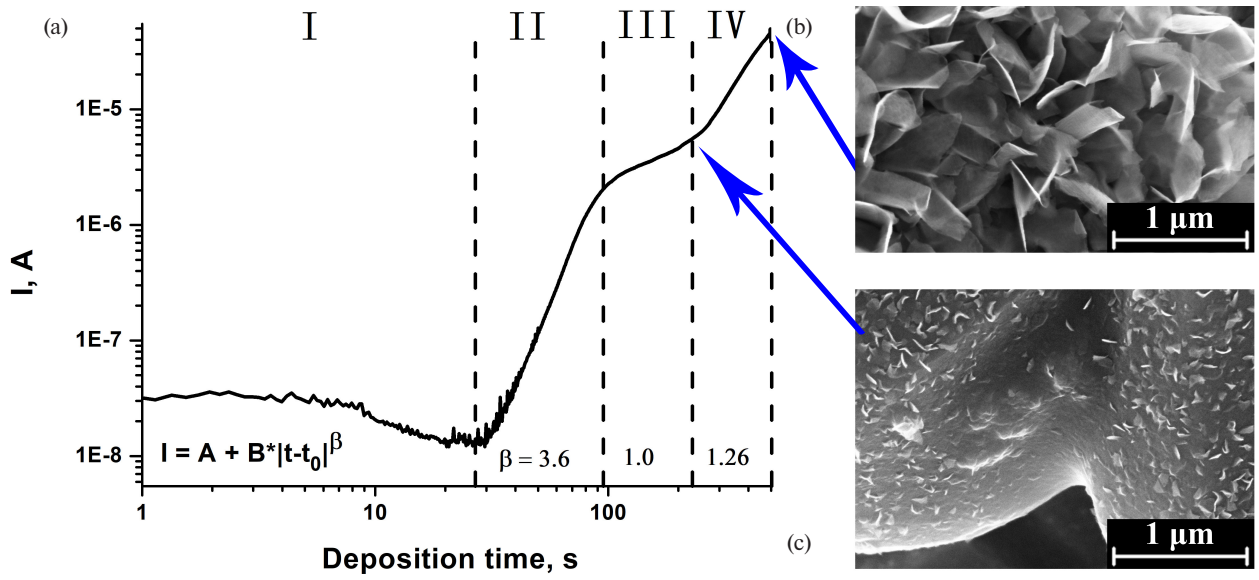

Fig. 7. *a* — Dependence of the current value between the contacts on the duration of deposition of the MoS_2 material. Current measurements were carried out at a constant applied voltage of 2.0 V between the Pt contacts. *b* and *c* are SEM images of films obtained at a deposition time of 500 and 120 seconds, respectively

at a wavelength of 655 nm, which is associated with the decay of the A^--exciton, and the intensity of the B-exciton peak decreases significantly.

A further increase in the duration of the precipitation leads to the fact that the intensity of the A-exciton peak increases by several orders of magnitude, and the peaks of B- and A^--exciton cease to be distinguishable against its background. The noted modification of the PL spectra can be explained by the fact that at the initial stages of film growth, the MoS_2 crystallites are located mainly parallel to the substrate, in contact with it with their entire plane. Such an arrangement is optimal for ensuring the interaction of the electronic subsystems of the crystallite and the substrate, which can lead to the creation of *n*-type conductivity in MoS_2 and, as a result, to a decrease in the intensity of the A-exciton peak of the PL [30,31].

With an increase in the deposition duration MoS_2 crystallites begin to form from linear defects at the boundaries of flat grains, oriented perpendicular to the surface, which are connected to the substrate not by the entire plane, but only by a small area at their end. The lack of effective contact with the substrate leads to a decrease in the degree of doping and, consequently, a decrease in the effectiveness of suppressing the intensity of the A-exciton PL band, i.e., to an increase in the intensity of this band with an increase in the size of vertically oriented crystallites. Figure 6b shows the dependence of the maximum intensity of PL (when normalizing the spectrum of PL on 408 cm^{-1} Raman spectroscopy line) on the deposition duration, which, as well as the dependence shown in Fig. 5*b*, has a non-monotonic character, reflecting the presence of various stages of formation of the MoS_2 material.

A further increase in the duration of deposition leads, as previously shown [23], to a thickening of vertically oriented crystallites, and a decrease in the intensity of PL due to the fact that MoS_2 ceases to be a straight-band semiconductor with an increase in the number of layers and electron transitions with photon radiation proceed at a lower rate [29].

In addition to the described studies of Raman spectroscopy and PL, measurements of the electrical conductivity of the formed MoS_2 material were carried out directly during the CVD process (*in situ*). To do this, two Pt contacts in the form of nested combs were applied to the surface of the Al_2O_3 substrate by an electrolytic method. During the measurement, the current was measured (using a Keithley 6487 picoammeter) between the platinum contacts at a constant applied voltage of 2 V. The graph of the dependence of the flowing current (conductivity) on the deposition time is shown in Fig. 7*a*. In this graph, 4 areas are clearly

distinguished, which indicate the presence of various stages of material formation. Region I is characterized by a minimum value of the flowing current, the value of which is determined by the intrinsic conductivity of the Al_2O_3 substrate.

In areas II, III, IV, highlighted in Fig. 7*a*, a change in the magnitude of the flowing current was observed, which can be approximated by degree dependencies with various indicators shown on the graph presented in double logarithmic coordinates. The presence of these 4 regions, depending on the change in the electrical conductivity of the deposited material from time to time, is consistent with the data on the change on the Raman spectroscopy (Fig. 5*b*) and PL (Fig. 6*b*). At the initial stage, corresponding to the region I in Fig. 7*a*, MoS_2 crystallites are being formed, isolated (including electrically) from each other. Accordingly, the electrical conductivity between the contacts on the substrate turns out to be minimal and unchanged until the moment when contact occurs between the separate crystallites and the first cluster of MoS_2 crystals connecting two electrical contacts is formed. At the stage of formation of the material corresponding to region II in Fig. 7*a*, the contact area between the individual crystallites increases, i.e. their gradual accretion and formation of a continuous film. After the first continuous channel of electric current flow from one electrical contact to another through the MoS_2 film is formed, the conductivity begins to increase sharply. The observed sharp increase in conductivity can be described using a percolation model of conductivity, in which the conductivity increases with an increase in the number of paths of electric current through the film [32].

This stage can be characterized by a power dependence with the index $\beta_{II} = 3.6 \pm 0.1$. At the stage of formation of the deposited material corresponding to region III in Fig. 7a, a further increase in electrical conductivity is determined by an increase in the thickness of the MoS_2-film. The recorded current value varies almost linearly with an increase in the deposition duration (the step index is $\beta_{III} = 1.0 \pm 0.2$). It can be noted that logical dependencies containing three stages could be obtained to change the conductivity for carbon nanotube films with an increase in their concentration [32]. Differences in the exponential dependences for nanotubes (see [32]) and MoS_2 plates (see Fig. 7a) are determined, apparently, by the fact that the contacts between the nanotubes are point-like, and for flat MoS_2 crystallites they are linear. In addition, during the formation of MoS_2 films, a stage corresponding to region IV in Fig. 7*a*, at which the increase in electrical conductivity can be explained by the formation of vertically oriented crystallites. The contact area of these crystallites increases with increasing duration of the deposition process, which leads to an increase in the exponential dependence of the amount of electric current flowing between the contacts: $\beta_{IV} = 1.266 \pm 0.003$.

After completion of the CVD process, accompanied by *in situ* measurement of film resistance, the morphology of the samples was analyzed using SEM. The corresponding SEM images for samples obtained with a synthesis duration of 500, 120 s are shown in Fig. 7 *a*, *b*. The morphology of the film obtained at a synthesis duration of 500 s (Fig. 7*b*) is identical to films obtained on substrates of other types (see Fig. 4). At a deposition duration of 120 s (Fig. 7c), noticeable differences are observed, determined, among other things, by the granular structure of the Al_2O_3 substrate material: vertically oriented MoS_2 crystallites are formed on the surface in the central part of the Al_2O_3 zone (the lateral part of the frame in Fig. 7*c*), however, at the boundary between the grains (in the center of the frame), the number of such crystallites is significantly smaller, and the film corresponds to the structure of MoS_2 with the crystalline orientation of the layers mainly parallel to the substrate surface.

This observation can be explained by the fact that with a constant flow of gaseous precursors on a surface inclined relative to it, the number of precursor molecules falling per unit area (hence the film growth rate) is less than on a surface perpendicular to the gas flow. Thus, in Fig. 7*c*, the film at the grain boundary is still at the final stage of formation of a continuous film, and the area far from the boundary is already at the stage of formation of vertically oriented crystallites.

Thus, the data obtained using various techniques (SEM, Raman spectroscopy, PL and *in situ* measurements of electrical conductivity) are consistent with each other and, in particular, indicate the presence of several stages in the formation of matter, which are schematically presented in Fig. 8 and include the following stages.

I. Formation of individual crystallites on the surface of the substrate. The atomic layers in the crystals are oriented parallel to the surface of the

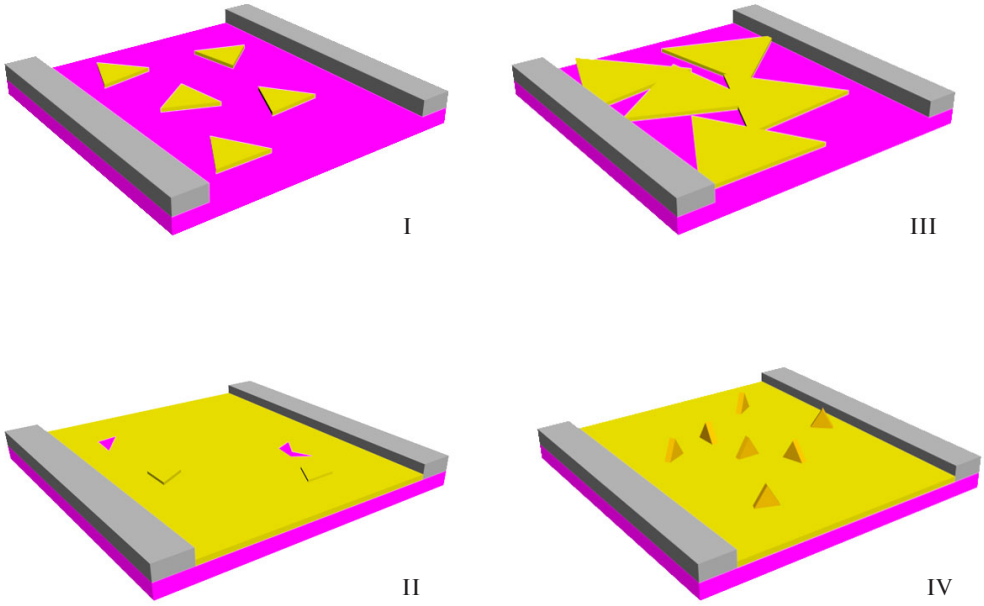

Fig. 8. Stages of growth of TMD films: I — formation of isolated islands; II — percolation stage III — formation of a continuous film; IV — nucleation and growth of vertically oriented crystallites

spoon. The absence of contacts between the crystals leads to a lack of electrical conductivity. In this case, good contact with the substrate leads to a redistribution of charges and doping of crystallites by electrons, which manifests itself in the predominance of bands of A^-- and B-excitons in the PL spectrum and suppression of the band associated with the A exciton. The thickness of such crystallites, in accordance with the data of the Raman spectroscopy is 2–3 atomic layers of MoS_2.

II. The union of crystallites growing along the surface of the substrate. The increase in the size of the crystals along the surface of the substrate leads to the appearance of contacts between them, including electrical ones. The resulting electrical conductivity increases with increasing deposition duration. However, the thickness of the individual crystallites remains similar to stage I (2–3 atomic layers).

III. An increase in the number of atomic layers in MoS_2 crystals forming a continuous film. The continuation of the deposition process leads to an increase in the thickness of the MoS_2 film, which is accompanied by an increase in its electrical conductivity and PL intensity, the absence of an A-exciton peak in the spectrum of which indicates a constant interaction with the substrate and effective electron doping.

IV. Formation and growth of MoS_2 crystallites oriented perpendicular to the substrate. Linear structural defects caused by contact of crystallites growing along the substrate surface serve as centers of formation of crystallites growing perpendicular to the substrate. The absence of direct contact with the substrate leads to the elimination of doping and the corresponding reduction of the A^--exciton peak in the PL spectrum. The thickness of vertically oriented crystals at the initial stages of their growth is 2–3 atomic layers. As the deposition duration increases, the thickness and lateral dimensions of the crystallites increase, which leads to a decrease in the intensity of the A- exciton peak and a shift in its position to the long-wave region (see [23]).

This model of growth and transition from the “lateral” morphology of films to the “vertical” can also be used to describe the deposition of other two-dimensional (layered) materials such as graphene, hexagonal boron nitride, etc.

4. CONCLUSION

As a result of the work carried out, data were obtained indicating the presence of several stages in the process of obtaining TMD materials during deposition from the gas phase. The observed changes in the PL spectra are consistent with the

proposed model for the formation of such materials in terms of explaining the manifestation of excitons of various types due to the interaction or absence of the formed MoS_2 and WS_2 TMD crystals with the substrate. A model has been developed for the growth of TMD films (such as MoS_2 and WS_2) during chemical deposition from the gas phase, in which gaseous hydrogen sulfide and thermally sprayed molybdenum or tungsten are used as precursors. The stages of film formation identified for MoS_2 and WS_2 include the following stages: 1) the formation of isolated crystalline islands; 2) the formation of contacts between expanding crystals; 3) the formation of a continuous polycrystalline film; 4) the formation and growth of vertically oriented crystallites. Morphological features of the films at these stages were revealed using raster electron microscopy (SEM). Based on the results of Raman and PL spectroscopy, it was found that the average number of layers in the crystallites of the film varies nonmonotonously. Until the film becomes solid, the crystallites consist of 2–3 layers, then the number of layers grows to 4–5. However, after the formation of vertically oriented crystallites, their thickness decreases again to 2–3 which is reflected in the position of the lines in the Raman spectra. The PL spectra also change qualitatively during film deposition. At the initial stages, the PL spectrum is dominated by lines associated with the recombination of A^--exciton and B-excitons, however, during the formation of vertical structures, a new peak appears associated with the recombination of A-exciton, against which the initial exciton peaks cease to be distinguishable after a certain deposition time. Measurements of the conductivity of the film during its deposition also confirm the described model. The dependence of conductivity on time corresponds to four stages, which can be compared with the film growth stages presented in the proposed growth model. The determination of the stages of formation of TMD films and the physical properties characteristic of each of the stages contribute to the development of technologies for the CVD synthesis of TMD materials with predetermined properties.

ACKNOWLEDGEMENT

The equipment of the Educational and Methodological Center of Lithography and Microscopy of Lomonosov Moscow State University was used in the work.

FUNDING

The study of the synthesis process is supported by the Russian Scientific Foundation (Grant No. 23-22-00132). Studies of the morphological properties of films were carried out with the support of the Foundation for the Development of Theoretical Physics and Mathematics “BASIS” (Grant No. 21-2-10-34-1). Optical study was carried out with the support of the Russian Science Foundation (Frant No. 21-72-20050).

REFERENCES

1. Manzeli S, Ovchinnikov D, Pasquier D, Yazyev O V and Kis A 2017 Nat. Rev. Mater. 2 17033
2. Chernozatonskii L A and Artyukh A A 2018 Phys.-Uspekhi 61 2–28
3. Bhimanapati G R, Lin Z, Meunier V, Jung Y, Cha J, Das S, Xiao D, Son Y, Strano M S, Cooper V R, Liang L, Louie S G, Ringe E, Zhou W, Kim S S, Naik R R, Sumpter B G, Terrones H, Xia F, Wang Y, Zhu J, Akinwande D, Alem N, Schuller J A, Schaak R E, Terrones M and Robinson J A 2015 ACS Nano 9 11509–39
4. Chowdhury T, Kim J, Sadler E C, Li C, Lee S W, Jo K, Xu W, Gracias D H, Drichko N V, Jariwala D, Brintlinger T H, Mueller T, Park H-G and Kempa T J 2020 Nat. Nanotechnol. 15 29–34 [5] Feng Y P, Shen L, Yang M, Wang A, Zeng M, Wu Q, Chintalapati S and Chang C 2017 WIREs Comput. Mol. Sci. 7
5. Schaibley J R, Yu H, Clark G, Rivera P, Ross J S, Seyler K L, Yao W and Xu X 2016 Nat. Rev. Mater. 1 16055
6. Wang T-H and Jeng H-T 2017 Npj Comput. Mater. 3 5
7. Yi Y, Chen Z, Yu X, Zhou Z and Li J 2019 Adv. Quantum Technol. 2 1800111
8. Lin Y, Ling X, Yu L, Huang S, Hsu A L, Lee Y-H, Kong J, Dresselhaus M S and Palacios T 2014 Nano Lett. 14 5569–76
9. Mak K F and Shan J 2016 Nat. Photonics 10 216–26
10. Bernardi M, Palummo M and Grossman J C 2013 Nano Lett 13
11. Liu H F, Wong S L and Chi D Z 2015 Chem. Vap. Depos. 21 241–59
12. Li S, Chen X, Liu F, Chen Y, Liu B, Deng W, An B, Chu F, Zhang G, Li S, Li X and Zhang Y 2019 ACS Appl. Mater. Interfaces 11 11636–44
13. Ma X, Zhang J, Sun Y, Wu C, Geng G, Zhang J, Wu E, Xu L, Wu S, Hu X and Liu J 2022 ACS Appl. Mater. Interfaces 14 47288–99

14. Peng X, Chen J, Wang S, Wang L, Duan S, Feng P and Chu J 2022 Appl. Surf. Sci. 599 153904 [16] Mobtakeri S, Habashyani S and Gür E 2022 ACS Appl. Mater. Interfaces 14 25741– 52
15. Sun J, Li X, Guo W, Zhao M, Fan X, Dong Y, Xu C, Deng J and Fu Y 2017 Crystals 7 198
16. Zhang X-Q, Lin C-H, Tseng Y-W, Huang K-H and Lee Y-H 2015 Nano Lett. 15 410– 5
17. Liu Y, Weiss N O, Duan X, Cheng H-C, Huang Y and Duan X 2016 Nat. Rev. Mater. 1 16042 [20] Sahoo P K, Memaran S, Xin Y, Balicas L and Gutiérrez H R 2018 Nature 553 63–7
18. Loginov A B, Fedotov P V, Bokova-Sirosh S N, Sapkov I V, Chmelenin D N, Ismagilov R R, Obraztsova E D, Loginov B A and Obraztsov A N 2022 Phys. Status Solidi B 2200481
19. Arzhakov M S, Aleksandrova N A, Zhirnov A E, Lukovkin G M and Arzhakov S A 2008 Dokl. Phys. Chem. 418 26–9
20. Wang S, Rong Y, Fan Y, Pacios M, Bhaskaran H, He K and Warner J H 2014 Chem. Mater. 26 6371–9
21. Godin K, Cupo C and Yang E-H 2017 Sci. Rep. 7 17798
22. Kleshch V I, Ismagilov R R, Mukhin V V, Orekhov A S, Filatyev A S and Obraztsov A N 2022 Nanotechnology 33 415201
23. Ismagilov R, Malykhin S, Puzyr A, Loginov A, Kleshch V and Obraztsov A 2021 Materials 14 2320
24. Lee C, Yan H, Brus L E, Heinz T F, Hone J and Ryu S 2010 ACS Nano 4 2695–700
25. Berkdemir A, Gutiérrez H R, Botello-Méndez A R, Perea-López N, Elías A L, Chia C-I, Wang B, Crespi V H, López-Urías F, Charlier J-C, Terrones H and Terrones M 2013 Sci. Rep. 3 1755
26. Do Nascimento Barbosa A, Mendoza C A D, Figueroa N J S, Terrones M and Freire Júnior F L 2021 Appl. Surf. Sci. 535 147685
27. Splendiani A, Sun L, Zhang Y, Li T, Kim J, Chim C-Y, Galli G and Wang F 2010 Nano Lett. 10 1271–5
28. Scheuschner N, Ochedowski O, Kaulitz A-M, Gillen R, Schleberger M and Maultzsch J 2014 Phys. Rev. B 89 125406
29. Zhu B, Chen X and Cui X 2015 Sci. Rep. 5 9218
30. Wang G, Chernikov A, Glazov M M, Heinz T F, Marie X, Amand T and Urbaszek B 2018 Rev. Mod. Phys. 90 021001
31. Salehi S and Saffarzadeh A 2016 Surf. Sci. 651 215–21
32. Mak K F, He K, Lee C, Lee G H, Hone J, Heinz T F and Shan J 2013 Nat. Mater. 12 207–11
33. Klots A R, Newaz A K M, Wang B, Prasai D, Krzyzanowska H, Lin J, Caudel D, Ghimire N J, Yan J, Ivanov B L, Velizhanin K A, Burger A, Mandrus D G, Tolk N H, Pantelides S T and Bolotin K I 2014 Sci. Rep. 4 6608
34. Lee B M and Loh K J 2015 J. Mater. Sci. 50 2973–83